Stabilization of the Transition State of the Chorismate-Prephenate Rearrangement: An ab Initio Study of Enzyme and Antibody Catalysis

Olaf Wiest‡ and K. N. Houk*

Contribution from the Department of Chemistry and Biochemistry, University of California, Los Angeles, California 90095-1569

Received June 12, 1995®

Abstract: The Claisen rearrangement of chorismate to prephenate and models for the catalysis of this reaction by the enzyme chorismate mutase were studied using Hartree-Fock and density functional theories. Substituent effects on the reaction are studied using several simple model systems. Whereas carboxylic acid or carboxylate substituents in the 2-position or a carboxylate in the 6-position of allyl vinyl ether leads to a lower activation energy, substitution by a carboxylic acid in the 6-position increases the activation energy. Upon 2,6-disubstitution, there is an increase in activation energy due to electrostatic repulsion between the carboxylates in the transition state. Similar results were obtained for substituted vinyl cyclohexadienyl ethers. Secondary kinetic isotope effects and substituent effects on reactant and transition state geometries are discussed. The catalysis of the reaction by the amino acid side chains in the enzyme was studied by calculation of the interaction of various functional groups that mimic the active site of chorismate mutase from *Bacillus subtilis* with substituted allyl vinyl ethers. Selective transition state binding by appropriately positioned hydrogen bond donors is the most important factor for catalysis, lowering the activation energy by 6 kcal/mol in the case of allyl vinyl ether-2,6-dicarboxylate. Charge complementarity to a 2-carboxylate and increased hydrogen-bonding to the ether oxygen lower the activation energy by 1.7 and 2 kcal/mol, respectively. Stabilization of the positive partial charge in the allyl part of the transition state has no significant catalytic effect. Electrophilic catalysis involving strong binding to the ether oxygen leads to a dissociative mechanism. The results are discussed with respect to the catalytic mechanism of the native enzymes and the antibody 1F7.

Introduction

The transformation of chorismate **1** to prephenate **2** is a key step in the biosynthesis of the aromatic amino acids phenylalanine and tyrosine in bacteria, fungi, and higher plants.[1] The reaction is the only [3,3]-sigmatropic shift reaction known to be catalyzed by an enzyme, chorismate mutase. The transformation is at least formally a Claisen rearrangement and occurs at a branch point of the shikimic acid pathway, making chorismate the last common intermediate in the biosynthesis of a multitude of aromatic compounds.[2] Chorismate mutases have been isolated from various organisms and have only poor homology.[3] The central position of this enzyme in lower organisms and its absence in mammals makes it an attractive target for the development of inhibitors, which could be of potential use as antibactericides, fungicides, and herbicides. The biology and the unique mechanism have led to extensive study of the chorismate-prephenate rearrangement over the last two decades. Mechanistic studies and crystallographic evidence about the enzyme structure have led to the conclusion that the enzyme catalyzed reaction has the same concerted [3,3]-sigmatropic shift mechanism as the uncatalyzed reaction. The reaction can also be accelerated by monoclonal catalytic antibodies that have been raised against a stable transition state analog.[4,5]

A thorough knowledge of the geometry and electronic structure of the transition state is the key to an understanding of the reaction and how it can be catalyzed.[6] This information is available through location of transition structures using quantum mechanical methods. Early calculations were reported on the chorismate rearrangement using EHT and MINDO/3 semiempirical methods.[7] Recently, ab initio methods have been used to study this reaction by our group[8] and others.[9] We have been able to show that the transition structure calculated at the RHF/6-31G* level of theory reproduces the experimental tritium kinetic isotope effects reasonably well. We have now explored the reaction with other basis sets and density functional theory (DFT) and have studied model systems to mimic the modes of catalysis that are used in the enzyme and the antibody to accelerate this reaction.

This paper begins with a brief review of the experimental data relevant to the present study. The second part reports new

‡ Current address: Department of Chemistry and Biochemistry, University of Notre Dame, Notre Dame, IN 46556.

® Abstract published in *Advance ACS Abstracts*, November 1, 1995.

(1) (a) Haslam, E. *Shikimic Acid Metabolism and Metabolites*; Wiley & Sons: New York, 1993. (b) Ganem, B. *Tetrahedron* **1978**, *34*, 3353-3383. (c) Weiss, U.; Edwards, J. M. *The Biosynthesis of Aromatic Amino Compounds*; Wiley & Sons: New York, 1980; pp 134-184.

(2) Edwards, J. M.; Jackman, L. M. *Aust. J. Chem.* **1965**, *18*, 1227-1239.

(3) E.g.: (a) Koch, G. L. E.; Shaw, D. C.; Gibson, F. *Biochem. Biophys. Acta* **1971**, *229*, 795-804. (b) Gray, J. V.; Golinelli-Pimpaneau, B.; Knowles, J. R. *Biochemistry* **1990**, *29*, 376-383. (c) Dopheide, T. A.; Crewther, P.; Davidson, B. E. *J. Biol. Chem.* **1972**, *247*, 4447-4452.

(4) (a) Hilvert, D.; Carpenter, S. H.; Nared, K. D.; Auditor, M.-T. M. *Proc. Natl. Acad. Sci. U.S.A.* **1988**, *85*, 4953-4955. (b) Hilvert, D.; Nared, K. D. *J. Am. Chem. Soc.* **1988**, *110*, 5593-5594. (c) Bowdish, K.; Tang, Y.; Hicks, J. B.; Hilvert, D. *J. Biol. Chem.* **1991**, *266*, 11901-11908. (d) Hilvert, D. *Acc. Chem. Res.* **1993**, *26*, 552-558. (e) Shin, J. A.; Hilvert, D. *Bioorg., Med. Chem. Lett.* **1994**, *4*, 2945-2948. (f) Campbell, A. P.; Tarasow, T. M.; Massefski, W.; Wright, P. E.; Hilvert, D. *Proc. Natl. Acad. Sci. U.S.A.* **1993**, *90*, 8663-8667.

(5) (a) Schultz, P. G. *Science* **1988**, *240*, 426-433. (b) Jackson, D. Y.; Jacobs, J.; Sugasawara, R.; Reich, S. H.; Bartlett, P. A.; Schultz, P. G. *J. Am. Chem. Soc.* **1988**, *110*, 4841-4842.

(6) Jencks, W. P. *Catalysis in Chemistry and Enzymology*; Dover: New York, 1987; pp 655-659.

(7) (a) Andrews, P. R.; Heyde, E. *J. Theor. Biol.* **1979**, *78*, 393-403. (b) Andrews, P. R., Haddon, R. C. *Aust. J. Chem.* **1979**, *32*, 1921-1929.

(8) Wiest, O.; Houk, K. N. *J. Org. Chem.* **1994**, *59*, 7582-7584.

(9) a) Davidson, M. M.; Hillier, I. H. *J. Chem. Soc., Perkin Trans. 2* **1994**, 1415-1417. (b) Davidson, M. M.; Hillier, I. H. *Chem. Phys. Lett.* **1994**, *225*, 293-296. (c) Davidson, M. M.; Gould, I. R.; Hillier, I. *J. Chem. Soc., Chem. Commun.* **1995**, 63-64.

0002-7863/95/1517-11628$09.00/0

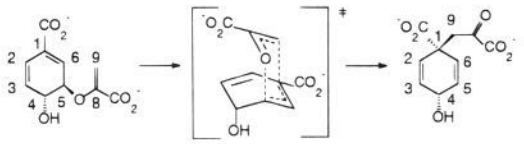

1 2

Figure 1. Claisen rearrangement of chorismate **1** to prephenate **2**.

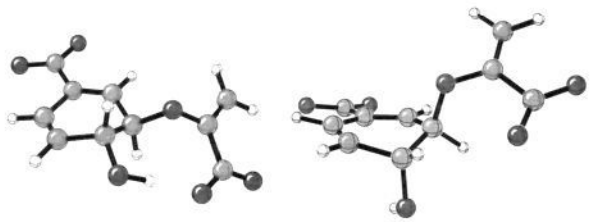

Figure 2. Pseudodiequatorial (left) and pseudodiaxial (right) conformation of chorismate **1**.

theoretical studies of the Claisen rearrangements of several small model systems for chorismate. This study establishes the level of theory necessary for the proper treatment of the reaction and gives information about the origin and magnitude of substituent effects in chorismate. The third section describes theoretical investigations of the catalysis of Claisen rearrangements of several model systems by appropriately positioned functional groups. These were chosen in order to mimic subunits of the three-dimensional structures of the enzyme and the antibody. From these studies, the quantitative contributions of specific interactions in the active sites were evaluated. Finally, we discuss the relevance of these model studies to the catalytic mechanisms in the enzymes and the antibodies.

Background

The activation parameters for the uncatalyzed reaction of chorismate to form prephenate at pH 7.5 are $\Delta H^{\ddagger} = 20.7 \pm 0.4$ kcal/mol and $\Delta S^{\ddagger} = -12.9 \pm 0.4$ eu.[10] The reaction is known to proceed via a chair-like transition state.[11] Bond breaking in the transition state is more advanced than bond making, as shown by the large tritium kinetic isotope effect of 1.149 ± 0.012 for the breaking bond (H-5) and the negligible effect of 0.992 ± 0.012 for the forming bond (H-9).[12] From the solvent dependence of the reaction rate[13] as well as from the studies of several model compounds,[14] it is clear that the transition state is considerably more polar than the reactant, although a dissociative mechanism with complete charge separation is unlikely.[15] Chorismate **1** can adopt several conformations. The pseudodiequatorial, shown on the left in Figure 2, is the most stable in all three phases.[8,13,16] The pseudodiaxial conformation

Table 1. Selected Data for Chorismate Mutase and Antibody 1F7

parameter[a]	uncatalyzed[10]	chorismate mutase[10]	1F7[4]
k_{cat} [s^{-1}]		50	0.0012
k_{cat}/k_{uncat}		1.9×10^6	190
K_m [M]		4.5×10^{-5}	5.1×10^{-5}
$(k_{cat}/K_m)/k_{uncat}$ [M^{-1}]		4.2×10^{10}	3.7×10^6
$\Delta H^{\ddagger}$ [kcal/mol]	20.5	15.9	15
$\Delta S^{\ddagger}$ [eu]	−12.9	0.0	−22
$\Delta G^{\ddagger}$ [kcal/mol]	24.2	15.9	21.3

[a] At 25 °C.

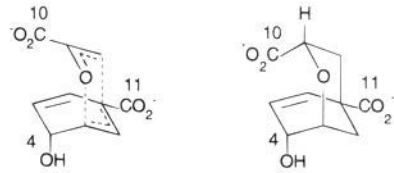

Figure 3. Transition state (left) and transition state analog **3** (right) of the Claisen rearrangement of chorismate.

is much closer in structure to the concerted transition state. The concentration of the pseudodiaxial conformation is also strongly solvent dependent.[13,17] In both, the pseudodiaxial conformer and in the transition state, the hydrogen bond between the side chain carboxylate and the hydroxyl group present in the pseudodiequatorial form of **1** is disrupted, and the two negatively charged carboxylates must be brought into closer proximity.

As can be seen in Table 1, the enzyme chorismate mutase accelerates the reaction by a factor of about 2×10^6 over the uncatalyzed reaction.[10] This large catalytic effect on a reaction that already proceeds readily at room temperature is achieved by simultaneously lowering $\Delta H^{\ddagger}$ to 15.9 kcal/mol and by increasing $\Delta S^{\ddagger}$ to virtually zero.[18] From the absence of the tritium kinetic isotope effects observed in the uncatalyzed reaction, it has been deduced that the rearrangement itself is not the rate determining step in the enzyme-catalyzed process.[12] Stereochemical studies using isotopically labeled substrates prove that the enzyme catalyzed reaction proceeds through a chair-like transition state.[11c,12] Indeed, the endo oxabicyclic transition structure analog **3**,[19] which mimics the geometry of the actual transition structure quite well,[8] has proven to be the most potent of a variety of chorismate mutase inhibitors tested so far.[20]

Several possible catalytic mechanisms have been proposed for chorismate mutase. Görisch suggested that there is binding of the pseudodiequatorial conformation of **1**, followed by a conformational change assisted by positively charged residues in the active site of the enzyme.[18] Based on the measurement of solvent kinetic isotope effects and the absence of a secondary kinetic isotope effect in the enzyme catalyzed reaction, Knowles et al. originally proposed a S_N2-S_N2' mechanism involving a nucleophilic attack at C-5.[21]

(10) Andrews, P. R.; Smith, G. D.; Young I. G. *Biochemistry* **1973**, *12*, 3492–3498.

(11) (a) Sogo, S. G.; Widlanski, T. S.; Hoare, J. H.; Grimshaw, C. E.; Berchtold, G. A.; Knowles, J. R. *J. Am. Chem. Soc.* **1984**, *106*, 2701–2703. (b) Asano, Y.; Lee, J. J.; Shieh, T. L.; Spreafico, F.; Kowal, C.; Floss, H. G. *J. Am. Chem. Soc.* **1985**, *107*, 4314–4320. (c) Knowles, J. R. *Pure Appl. Chem.* **1984**, *56*, 1005–1010.

(12) Addadi, L.; Jaffe, E. K.; Knowles, J. R. *Biochemistry* **1983**, *22*, 4494–4501.

(13) Copley, S. D.; Knowles, J. R. *J. Am. Chem. Soc.* **1987**, *109*, 5308–5013.

(14) (a) Gajewski, J. J.; Jurayj, J.; Kimbrough, D. R.; Gande, M. E.; Ganem, B.; Carpenter; B. E. *J. Am. Chem. Soc.* **1987**, *109*, 1170–1186. (b) Coates, R. M.; Rogers, B. D.; Hobbs, S. J.; Peck, D. R.; Curran, D. P. *J. Am. Chem. Soc.* **1987**, *109*, 1160–1170.

(15) Gajewski, J. J.; Brichford, N. L. *J. Am. Chem. Soc.* **1994**, *116*, 3165–3166.

(16) Afshar, C.; Jaffe, E. K.; Carrell, H. L.; Markham, G. D.; Rajagopalan, J. S.; Rossi, M.; Glusker, J. P. *Bioorg. Chem.* **1992**, *20*, 323–333.

(17) Batterham, T. J.; Young, I. G. *Tetrahedron Lett.* **1969**, *12*, 945–948.

(18) Görisch, H. *Biochemistry* **1978**, *17*, 3700–3705.

(19) (a) Bartlett, P. A.; Johnson, C. R. *J. Am. Chem. Soc.* **1985**, *107*, 7792–7793. (b) Smith, W. W.; Bartlett, P. A. *J. Org. Chem.* **1993**, *58*, 7308–7309. (c) Gray, J. V.; Eren, D.; Knowles, J. R. *Biochemistry* **1990**, *29*, 8872–8878. (d) Clarke, T.; Stewart, J. D.; Ganem, B. *Tetrahedron Lett.* **1987**, *28*, 6253–6256.

(20) (a) Andrews, P. R.; Cain, E. N.; Rizzardo, E.; Smith, G. D. *Biochemistry* **1977**, *16*, 4848–4852. (b) Chao, H. S.-I.; Berchtold, G. A. *Biochemistry* **1982**, *21*, 2778–2781. (c) Ife, R. J.; Ball, L. F.; Lowe, P.; Haslam, E. *J. Chem. Soc., Perkin Trans. 1* **1976**, 1776–1783. (d) Wood, H. B.; Buser, H.-P.; Ganem, B.; *J. Org. Chem.* **1992**, *57*, 178–184. (e) Bartlett, P. A.; Nakagawa, Y.; Johnson, C. R.; Reich, S. H.; Luis, A. *J. Org. Chem.*, **1988**, *53*, 3195–3210.

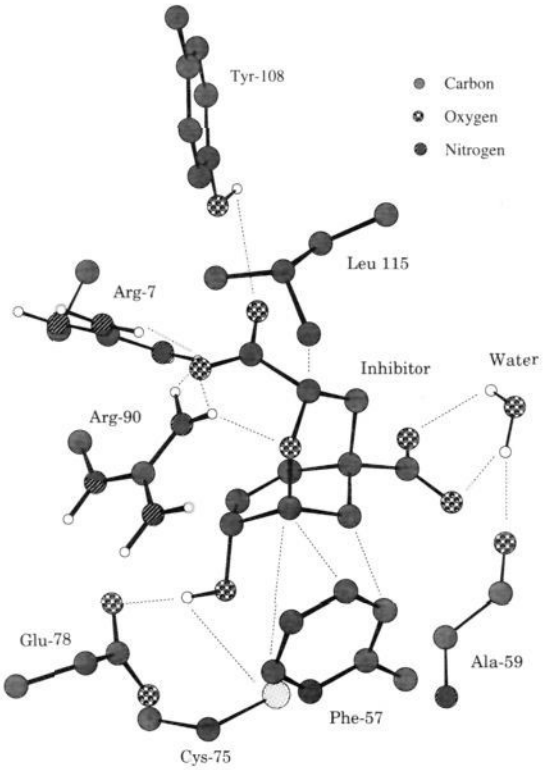

Figure 4. Active site of chorismate mutase from *Bacillus subtilis*.[22]

Recently, the three-dimensional structure of the monofunctional chorismate mutase from *Bacillus subtilis*, complexed with the transition state analog **3**, has been determined by X-ray crystallography.[22] Figure 4 shows a view of the active site with the bound transition state analog.[23] Although there are several contacts between amino acid side chains and the transition state analog, the following interactions are likely to be important for catalysis. The carboxylate at C-10 has polar interactions with Tyr-108 and ionic interactions with Arg-7 and Arg-90. The latter also seems to form a hydrogen bond to the ether oxygen. The carboxylate at C-11 points toward the solvent accessible surface of the protein and has only polar interactions with a water molecule. The hydroxyl group at C-4 forms several hydrogen bonds with the carboxylate of Glu-78 and the sulfur of Cys-75 as acceptors. There are hydrophobic interactions between the cyclohexenyl part of **3** and Phe-57 and between the CH_2CHO bridge of the inhibitor and Leu-115. From an analysis of the active site,[22,24] it is clear that the enzyme selectively binds a pseudodiaxial conformation where the side chain vinyl group points toward the ring, thus resembling the transition state conformation. Nucleophilic attack by an amino acid residue at C-5 is unlikely, since there is a reactive functional group in close proximity to this center. Based on the measured pH-profile of the enzyme catalyzed reaction, protonation of the ether oxygen was proposed as a possible mechanism for catalysis,[25] but this proposal was later rejected based on inhibitor studies.[26] A similar electrophilic catalysis by Arg-90, involving a dissociative transition state, has been ruled out by a recent FTIR study,[19c,27] where it was shown that the carbonyl group of prephenate has similar interactions in water and in the active site of the enzyme. It is therefore very likely that the enzyme catalyzed reaction has the same pericyclic mechanism as the uncatalyzed reaction. The three-dimensional structure of a mutant chorismate mutase from yeast, which shows a different overall structure than the one from *B. subtilis*, has also been described.[28] Although the active site was not located in this study, comparison of the three-dimensional structure of the yeast chorismate mutase with the one from *Eschericia coli* suggests that the active sites are very similar.[29] The active site of chorismate from *E. coli*, which has been published after the completion of the present study, will be discussed in a later section.

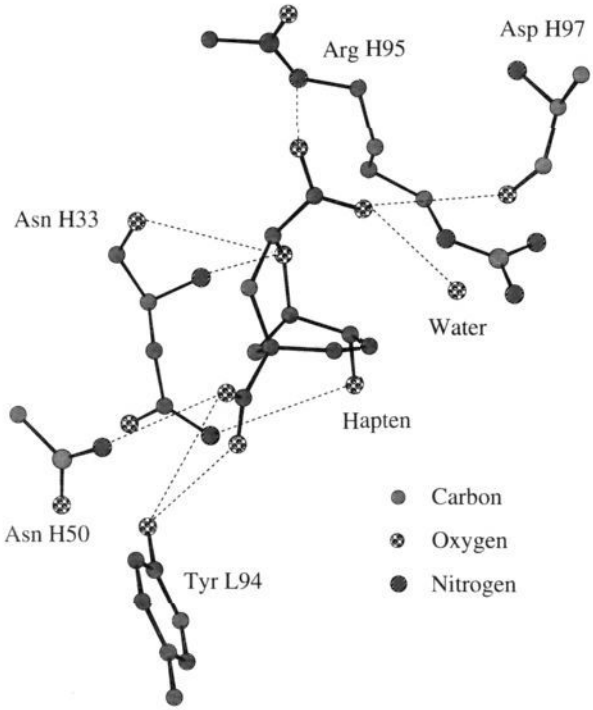

Figure 5. Active site of the catalytic antibody 1F7.[31b]

The transition state analog **3** has also been used to elicit two monoclonal catalytic antibodies with chorismate mutase activity. One of the antibodies, 1F7,[4] accelerates the rearrangement by a factor of 190 through lowering of the activation enthalpy to $\Delta H^{\ddagger} = 15 \pm 2$ kcal/mol), while the activation entropy ($\Delta S^{\ddagger} = -22 \pm 6$ eu) is more unfavorable than for the uncatalyzed reaction. The other antibody, 11F1−2E11, catalyzes the reaction by a factor of about 10^4 through a slight decrease of the activation enthalpy ($\Delta H^{\ddagger} = 18.3$ kcal/mol), while the activation entropy is increased to essentially zero ($\Delta S^{\ddagger} = -1.2$ eu).[30]

The three-dimensional structure of the antibody 1F7 bound to the hapten has been determined recently.[31] The active site is shown in Figure 5.[32] It shows considerable fewer interactions

(21) Guilford, W. J.; Copley, S. D.; Knowles, J. R. *J. Am. Chem. Soc.* **1987**, *109*, 5013−5019.
(22) Chook, Y. M.; Ke, H.; Lipscomb, W. N. *Proc. Natl. Acad. Sci. U.S.A.* **1993**, *90*, 8600−8603.
(23) Wiest, O.; Houk, K. N. *Chemtracts Org. Chem.* **1994**, *7*, 45−48.
(24) Chook, Y. M.; Gray, J. V.; Ke, H.; Lipscomb, W. N. *J. Mol. Biol.* **1994**, *240*, 476−500.
(25) Turnbull, J.; Cleland, W. W.; Morrison, J. F. *Biochemistry* **1991**, *30*, 7777−7782.
(26) Hediger, M. E. Ph.D. Dissertation, University of California at Berkeley, 1993.
(27) Gray, J. V.; Knowles, J. R. *Biochemistry* **1994**, *33*, 9953−9959.
(28) (a) Xue, Y.; Lipscomb, W. N. *J. Mol. Biol.* **1994**, *241*, 273−274. (b) Xue, Y.; Lipscomb, W. N.; Graf, R.; Schnappauf, G.; Braus, G. *Proc. Natl. Acad. Sci. U.S.A.* **1994**, *91*, 10814−10818.
(29) (a) Lee, A. Y.; Karplus, P. A., Ganem, B.; Clardy, J. *J. Am. Chem. Soc.* **1995**, *117*, 3627−3628. (b) Lee, A. Y.; Stewart, J. D.; Clardy, J.; Ganem, B. *Chem & Biol.* **1995**, *2*, 195−203. (c) Clardy, J. Ernest Guenther Award Address, 209th National ACS Meeting, Annaheim, CA, 5. April 1995, ORG217.
(30) Jackson, D. Y.; Liang, M. N.; Bartlett, P. A.; Schultz, P. G. *Angew. Chem.* **1992**, 104, 196−198; *Angew. Chem., Int. Ed. Engl.* **1992**, *31*, 182−184.

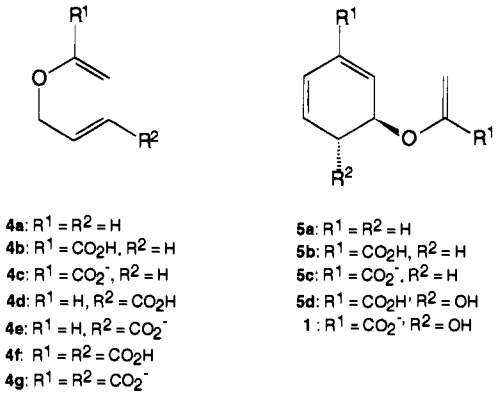

Figure 6. Model systems studied.

between the hapten and the binding site than found in the active site of the enzyme. Most contacts involve the amino acid backbone, such as the interactions of the carboxylate at C-10 with Arg-H95 and Asp-H97. The carboxylate at C-11 has several interactions with Tyr-L94 and Asn-H50, while the hydroxyl group at C-4 has only one contact with Asn-H33. Another feature of the active site of the antibody is that it has considerably fewer charged residues than its counterpart in the enzyme. This is particularly true for the environment of carboxylate at C-10 and the ether oxygen, which is strongly positive charged in the active site of the enzyme.[33] In spite of the smaller number of charge interactions possible to stabilize the transition state, the measured $\Delta H^{\ddagger}$ is as low as that for the enzyme. This may arise from the necessity of restricting the motion of the stabilizing groups in order to achieve transition state stabilization. Alternatively, the chorismate can be bound in the diequatorial conformation so that the antibody catalyzed and the uncatalyzed reaction both have the same unfavorable $\Delta S^{\ddagger}$. However, Hilvert et al. obtained some NMR spectroscopic evidence for binding of the chorismate in a diaxial conformation.[4]

Computational Methodology

All calculations have been carried out with the GAUSSIAN[34] and GAMESS[35] series of programs using the RHF and the BLYP[36] methods using the basis sets discussed below. All structures reported were fully optimized unless otherwise noted and were characterized by harmonic frequency analysis. The reported energies include zero point energies. All distances given are in Å. Atomic charges have been calculated using the CHELPG method;[37] and hydrogens have been summed into the heavy atoms. Kinetic isotope effects were calculated from the ab initio force constants using the program QUIVER.[38]

Table 2. Energies and Geometry Data for the Claisen Rearrangement of **4a–g** (RHF/6-31G*)

	reactant	transition structure			
compd	E [hartree]	E_a [kcal/mol]	E_a^{rel} [kcal/mol]	R_{C-O} [Å]	R_{C-C} [Å]
4a	−268.667 46	47.4	0.0	1.918	2.266
4b	−456.263 92	43.1	−4.3	1.942	2.249
4c	−455.704 86	40.7	−6.7	1.827	2.193
4d	−456.270 53	48.8	+1.4	1.934	2.281
4e	−455.710 64	40.7	−6.7	2.003	2.375
4f	−643.988 61	47.0	+0.4	1.952	2.300
4g	−642.677 37	51.3	+3.9	1.930	2.256

Table 3. Energies and Geometry Data for the Claisen Rearrangement of **4a–g** (RHF/6-31+G*)

	reactant	transition structure			
compd	E [hartree]	E_a [kcal/mol]	E_a^{rel} [kcal/mol]	R_{C-O} [Å]	R_{C-C} [Å]
4a	−268.675 59	46.2	0.0	1.940	2.296
4b	−456.278 04	43.1	−3.1	1.965	2.274
4c	−455.734 03	40.5	−5.7	1.846	2.216
4d	−456.285 32	48.7	+2.5	1.950	2.301
4e	−455.741 21	40.4	−5.6	2.033	2.412
4f	−643.888 03	47.1	+0.9	1.968	2.275
4g	−642.730 59	51.2	+5.0	1.953	2.334

Frequencies from RHF calculations were scaled by 0.91, and frequencies from density functional theory calculations were unscaled.[39]

Model Systems

Model systems **4** and **5** (Figure 6) were studied at different levels of theory in order to obtain insights into the substituent effects on the Claisen rearrangement of chorismate and to provide tractable model systems for studies of catalysis. Three different methods have been used. The results from the RHF/6-31G* calculations are shown in Table 2. For a proper description of anions, it is often necessary to supplement the basis set with a set of diffuse s- and p-functions.[40] We have, therefore, also performed RHF/6-31+G* calculations, which are summarized in Table 3. Finally, we studied the reaction using density functional theory, using the nonlocal BLYP/6-31G* method, which includes electron correlation effects. It has been shown that nonlocal DFT methods yield excellent activation energies and kinetic isotope effects (KIEs) in the case of the parent Claisen rearrangement as well as in a variety of hydrocarbon pericyclic reactions.[39,41] The results from the BLYP/6-31G* calculations are shown in Table 4. All three methods predict a loose, aromatic-type transition state. The calculated lengths of the breaking C–O bond range from 1.83–2.11 Å, and the lengths of the forming C–C bonds range from 2.19–2.70 Å. In accordance with earlier findings,[41,42] the bond lengths calculated by the BLYP/6-31G* method are systematically longer than the ones from RHF calculations. Interestingly, this trend is much more pronounced for the anions **4c**, **e**, and **g**.

(31) (a) Haynes, M. R.; Stura, E. A.; Hilvert, D.; Wilson, I. A. *Proteins* **1994**, *18*, 198–200. (b) Haynes, M. R.; Stura, E. A.; Hilvert, D.; Wilson, I. A. *Science* **1994**, *263*, 646–652.

(32) Wiest, O.; Houk, K. N. *Chemtracts Org. Chem.* in press.

(33) Inhibitor studies suggest that the active site of chorismate mutase from *Strepomyces aureofaciens* is also positively charged: ref 18.

(34) GAUSSIAN92 Revisions B and G.1; Frisch, M. J.; Trucks, G. W.; Head-Gordon, M.; Gill, P. M. W, Wong, M. W.; Foresman, J. W.; Johnson, B. G.; Schlegel, H. B.; Robb, M. A.; Replogle, E. S.; Gomberts, R.; Andres, J. L.; Raghavachari, K.; Binkley, J. S.; Gonzales, C.; Martin, R. L.; Fox, D. J.; Defrees, D. J.; Baker, J.; Stewart, J. J. P.; Pople, J. A. Gaussian Inc.: Pittsburgh, PA, 1992 and 1993.

(35) GAMESS Version 3/93; Schmidt, M. W.; Baldridge, K. K.; Boatz, J. S.; Jensen, J. H.; Koseki, S.; Gordon, M. S.; Nguyen, K. A.; Windus, T. L.; Elbert, S. T. *QCPE Bulletin* **1990**, *10*, 52–54.

(36) (a) Becke, A. D. *Phys. Rev. A* **1988**, *38*, 3098–3100. (b) Lee, C.; Yang, W.; Parr, R. G. *Phys. Rev. B* **1988**, *37*, 785–789.

(37) Breneman, C. M.; Wiberg, K. B. *J. Comput. Chem.* **1990**, *11*, 361–373.

(38) Saunders, M.; Laidig, K. E.; Wolfsberg, M. *J. Am. Chem. Soc.* **1989**, *111*, 8989–8994.

(39) Wiest, O.; Houk, K. N.; Black, K. A.; Thomas IV, B. E. *J. Am. Chem. Soc.* **1995**, *117*, 8594–8599.

(40) Hehre, W. J.; Radom, L.; Schleyer, P. v. R.; Pople, J. A. *Ab Initio Molecular Orbital Theory*; Wiley-Interscience: New York, 1986; pp 86–88, 310–316.

(41) Wiest, O.; Black, K. A.; Houk, K. N. *J. Am. Chem. Soc.* **1994**, *116*, 10336–10337.

(42) (a) Stanton, R. V. Merz, K. *J. Chem. Phys.* 1994, 100, 434–443. (b) Sosa, C. P.; Andzelm, J.; Lee, C.; Blake, J. F.; Chenard, B. L.; Butler, T. W. *Int. J. Quant. Chem.* **1994**, *49*, 511–526. (c) Carpenter, J. E.; Sosa, C. P. *J. Mol. Struct. (Theochem)* **1994**, *117*, 325–330. (d) Baker, J.; Muir, M.; Andzelm, J. *J. Chem. Phys.* **1995**, *102*, 2063–2079.

Table 4. Energies and Geometry Data for the Claisen Rearrangement of **4a**–**g** (BLYP/6-31G*)

	reactant	transition structure			
compd	E [hartree]	E_a [kcal/mol]	E_a^{rel} [kcal/mol]	R_{C-O} [Å]	R_{C-C} [Å]
4a	−270.268 84	21.1	0.0	1.959	2.428
4b	−458.799 44	19.0	−2.1	1.938	2.344
4c	−458.242 19	15.0	−6.1	1.898	2.384
4d	−458.803 24	21.0	−0.1	2.027	2.463
4e	−458.248 45	14.0	−7.1	2.112	2.698
4f	−647.332 98	20.3	−0.8	2.027	2.388
4g	−646.143 63	25.1	+4.0	2.073	2.575

The results from the RHF calculations using the 6-31G* and the 6-31+G* basis sets are quite similar with the bond lengths from the latter being about 0.02 Å longer for both, acids and anions. Therefore, the additional diffuse functions have a very small effect on the geometries obtained. The predicted substituent effects are qualitatively similar for all methods used, with a few notable exceptions. We discuss first the geometry changes upon substitution and then the effects on the activation energies.

As compared with the parent system, allyl vinyl ether, **4a**, substitution with a carboxylic acid in the 2- or 6-position leads to only small changes ($|\Delta r| \leq 0.03$ Å) in the geometry of the transition structures computed. Two exceptions are predicted by BLYP/6-31G*: substitution of the 6-position in **4d** leads to a significant increase of the length of the breaking bond, while carboxylic acid substitution in the 2-position of **4b** causes shortening of the forming C−C bond. The 2,6-diacid, **4f**, shows both effects.

The substituent effects on geometries are much more pronounced for the anion and dianion. After the deprotonation of **4b** to **4c**, a much tighter transition structure is predicted by all methods. The shortening of the forming and breaking bonds predicted by the BLYP/6-31G* method is less than found by RHF.

At the 6-position, all methods tested predict the transition structure to become much looser upon deprotonation. The length of the breaking C−O bond increases by about 0.08 Å independent of the method used. In contrast, the increase of the length of the forming bond predicted by the RHF methods (~0.1 Å) is quite different from the large increase of 0.24 Å predicted by the BLYP/6-31G* method. For the deprotonation of the diacid, **4f**, to form the dianion, **4g**, the substituent effects on geometries cancel each other out. Consequently, only small changes are predicted by the RHF methods, except for an 0.06 Å increase of the bond lengths of the forming bond computed at the RHF/6-31+G* level. This can be attributed to a better description of the electrostatic repulsion of the two carboxylates with the 6-31+G* basis set. With the BLYP/6-31G* method, considerably longer bonds are calculated for **4g**.

RHF methods overestimate the activation energy for the Claisen[43] and other pericyclic rearrangements.[44] The activation energies calculated for **4a** are considerably higher than the experimental value of 30.6 kcal/mol.[45] The BLYP method, on the other hand, underestimates the activation energies. Nevertheless, it is interesting to note that relative activation energies for all three methods follow the same pattern and give reasonable estimates of substituent effects on the energies of activation. The carboxyl substituent in 2-position of **4b** lowers the activation energy by about 3 kcal/mol in good agreement with the difference in activation energies between the parent allyl vinyl ether and 2-carboxymethoxyvinyl allyl ether.[14a] The substantial activation energy lowering arises from the stabilization of the developing partial negative charge on the enolate group in the transition state. Upon deprotonation of the carboxylic acid to **4c**, the activation energy is lowered by an additional 2.5 kcal/mol (4 kcal/mol at the BLYP/6-31G* level). The carboxylate anion is a weaker electron-withdrawing substituent than the carboxylic acid; however, the transition state is more polarizable than the reactant and can better stabilize the negative charge of the carbocylate.

The 6-carboxylic acid group raises the activation energy by 0−2.5 kcal/mol according to the RHF method, because the carboxyl group at C-6 stabilizes the ground state more than the transition state. This effect is negligible in the BLYP/6-31G* calculations, and the activation energy calculated for **4d** is the same as the one of **4a**. The higher activation energy of **4d** is in accordance with the fact that the methyl ester of **4d** does not rearrange at 100 °C, whereas **4a** rearranges at 80 °C with a rate constant of 0.649×10^{-6} s^{-1}.[14a] The relative rate constants of 111:1:0.11 for allyl vinyl ether 2-carbonitrile, **4a**, and allyl vinyl ether 6-carbonitrile in di-*n*-butyl ether[45b] are also in good agreement with the calculated values. The comparison of the theoretical substituent effects for **4b** and **4d** with the experimental values for the corresponding carbonitriles shows that the effect of the nitriles is primarily due to the electron withdrawing properties, as postulated earlier.[45b]

Deprotonation of **4d** results in a very large stabilization of the transition state. The activation energy is lowered by 6−7 kcal/mol. The large transition state stabilization in **4c** and **4e** can arise from interaction of the carboxylate anion with the positive partial charge in the allylic part of the transition state. Alternatively, the computed transition state stabilization might be a consequence of the higher polarizability of the aromatic-type transition state as compared to the reactant. This leads to a stronger interaction of a charge in close proximity with the delocalized π-electrons of the rearranging system. Similar results have been obtained for various pericyclic reactions of hydrocarbons by complexed lithium ions,[46] leading to lowering of the activation energies by 5−8 kcal/mol. High level *ab initio* calculations for these systems show that the reason for the acceleration is the greater electrostatic stabilization of the transition states as compared to the reactants. In the case of [1,5]-hydrogen shifts, it was also found that this effect depends on the position of the charge relative to the migrating hydrogen.[46]

The 2,6-disubstituted compound **4f** has an activation energy close to that of **4a** due to the cancellation of effects of the 2- and 6-carboxyl groups. If the effects of the acid groups at the 2- and 6-positions were additive, the activation energy would be 1−2 kcal/mol below that of **4a**. The computed values are ~1 kcal/mol above the calculated activation energies for **4a** by the RHF methods (1 kcal/mol below by the BLYP method). Dianion **4g** has a very large activation energy due to destabilization of the transition state by electrostatic repulsion between the two carboxylate groups in the transition state. If the individual effects of the carboxylates were additive, the activation energy of **4g** would be 11−13 kcal/mol *below* that of **4a**.

(43) (a) Vance, R. L.; Rondan, N. G.; Houk, K. N.; Jensen, F.; Borden, W. T.; Komornicki, A.; Wimmer, E. *J. Am. Chem. Soc.* **1988**, *110*, 2314−2315. (b) Yoo, H. Y.; Houk, K. N. *J. Am. Chem. Soc.* **1994**, *116*, 12047−12048.

(44) Houk, K. N.; Li, Y.; Evanseck, J. D. *Angew. Chem., Int. Ed. Engl.* **1992**, *31*, 682−708.

(45) (a) Schuler, F. W.; Murphy, G. W. *J. Am. Chem. Soc.* **1950**, *72*, 3155−3159. Compare also: (b) Burrows, C. J.; Carpenter, B. K. *J. Am. Chem. Soc.* **1981**, *103*, 6983−6984 and ref 14b.

(46) (a) Jiao, H.; Schleyer, P. v. R.; *Angew. Chem., Int. Ed. Engl.* **1993**, *32*, 1760−1763. (b) Jiao, H.; Schleyer, P. v. R. *J. Chem. Soc., Faraday Trans.* **1994**, *90*, 1559−1567.

Table 5. Theoretical and Experimental SKIEs for **4a** and **4b**

	4a			4b			
isotopomer	RHF/6-31G* [a]	BLYP/6-31G* [a]	experiment[a,48]	RHF/6-31G* [b]	RHF/6-31+G* [b]	BLYP/6-31G* [b]	experiment[b,c,48]
^{14}C-1	1.025	1.017		1.0308	1.0311	1.0269	1.0280 ± 0.0009
^{14}C-2	1.005	1.002	1.027 ± 0.0007	0.9992	0.9996	0.9984	1.0087 ± 0.0009
^{14}O-3	1.032	1.024	1.050 ± 0.0007	1.0350	1.0357	1.0324	
^{14}C-4	1.053	1.039	1.072 ± 0.0008	1.0625	1.0620	1.0554	1.0330 ± 0.0009
^{14}C-6	1.028	1.023	1.0178 ± 0.0007	1.0332	1.0328	1.0299	1.0118 ± 0.0009
(^{2}H-4)	1.053	1.059	1.092 ± 0.005	1.170	1.181	1.148	1.12
(^{2}H-6)$_2$	0.932	0.969	0.976 ± 0.005	0.874	0.876	0.913	0.91

[a] At 443.15 K. [b] Heavy atom KIE at 353.15 K, deuterium KIE at 334.65 K. [c] For 2-carboxymethoxyvinyl allyl ether.

Table 6. Energies and Geometry Data for the Claisen Rearrangement of **5a–d** and **1** (RHF/6-31G*)

	reactant$_{dieq}$	reactant$_{diax}$	transition structure				exp E_a^{rel} [a]
compd	E [hartree]	ΔE [hartree]	E_a [kcal/mol]	E_a^{rel} [a] [kcal/mol]	R_{C-O} [Å]	R_{C-C} [Å]	[kcal/mol]
5a	−383.38577	0.8	44.4	−3.0	2.068	2.449	−3.8
5b	−758.58879	0.4	44.9	−2.5	2.146	2.462	−2.8[b]
5c	−757.40658	1.8	57.0	+9.6	2.073	2.482	
5d[8]	−833.43751	5.7	50.4	+3.0	2.076	2.408	−2.0[b]
1[8]	−832.45491	15.8	67.8	+20.4	2.032	2.446	

[a] Relative to **4a**. [b] For the corresponding dimethyl ester.

Table 7. Energies and Geometry Data for the Claisen Rearrangement of **5a–d** and **1** (BLYP/6-31G*)

	reactant$_{dieq}$	reactant$_{diax}$	transition structure				exp E_a^{rel} [a]
compd	E [hartree]	ΔE [hartree]	E_a [kcal/mol]	E_a^{rel} [a] [kcal/mol]	R_{C-O} [Å]	R_{C-C} [Å]	[kcal/mol]
5a	−385.690 53	−0.6	16.9	−4.2	2.187	2.706	−3.8
5b	−762.753 44	−1.4	13.8	−7.3	2.376	2.680	−2.8[b]
5c	−761.576 72	0.6	24.3	+3.2	2.680	2.735	
5d	−837.952 88	1.9	18.9	−2.2	2.237	2.645	−2.0[b]
1	−836.795 68	11.7	34.3	+13.2	2.769	2.772	

[a] Relative to **4a**. [b] For the corresponding dimethyl ester.

These results immediately suggest an important way in which catalysis of such reactions is possible. Charged groups such as carboxylates can cause substantial acceleration of a pericyclic process, because of the higher polarizability of the transition state. In a multiply-charged system, this effect may be eliminated by changes in electron repulsion between like-charged groups. In such a case, ion-pairing with the charged groups can be helpful in reducing the mutual repulsion, although this may reduce the potential for transition state stabilization by charge-polarization effects. Future studies will elucidate the utility of this promising concept for the catalysis of pericyclic reactions.

One of the few experimental methods to obtain information about the transition state geometry is the measurement of kinetic isotope effects (KIEs). Comparison of the experimental with theoretical KIEs from ab initio calculations is an important tool for validation of theoretical methods and interpretation of transition states.[39,47] Of the model systems **4a–g**, only the KIEs of **4a** and 2-carboxymethoxyvinyl allyl ether,[48] for which **4b** can be used as a model, have been determined. The KIEs of **4a** have been discussed elsewhere[41] and are given along with those of **4b** in Table 5. The results from the RHF calculations are again very similar and differ by less than 1%. The KIEs calculated are systematically too high, whereas the results from the BLYP/6-31G* calculations are in much better agreement with the experimental results. Assuming that the replacement of the carboxylic acid in **4b** by the corresponding methyl ester has no significant effect on the transition state, the actual transition state is better described by the loose BLYP/6-31G* transition structure than by the tighter RHF structure. The theoretical primary KIEs at C-1 and the secondary KIEs at C-6 are very close to the experimental values, indicating that the length of the forming bond in the transition state is close to the calculated value of 2.344 Å. The primary KIE computed for C-6 is ~2% smaller than the experimental value. It should be noted that it has been found earlier that the slope of a plot of calculated KIE versus bond distances is close to 1 for this position.[41] The theoretical primary and secondary KIE at C-4 are too large, indicating that the length of the breaking bond is presumably slightly shorter than the calculated value of 1.938 Å.

We next undertook studies of systems containing the remaining features present in chorismate. Because the additional diffuse s and p functions do not have a significant effect on the results of the RHF calculations, the model systems **5a–d** and chorismate **1** have only been studied using the 6-31G* basis set and the RHF and BLYP methods. The results from these calculations are summarized in Tables 6 and 7. The transition structures calculated by both methods are much looser than the ones for the model systems **4** because of the stabilization of the allylic system by the cyclohexadienyl moiety. This favors a more dissociative transition structure and is in accord with the fact the second double bond in the cyclohexene ring system accelerates the reaction substantially.[14a,49] The transition structures of the acids **5b** and **5d** calculated by the BLYP method are about 0.2 Å looser than the ones from the RHF calculations,

(47) (a) Houk, K. N.; Black, K. A.; Gustafson, S. *J. Am. Chem. Soc.* **1992**, *114*, 8565–8572. (b) Storer, J. W. Raimondi, L.; Houk, K. N. *J. Am. Chem. Soc.* **1994**, *116*, 9675–9683 and references cites therein.

(48) (a) Kupzcyk-Subotkowska, L.; Saunders, W. H., Jr.; Shine, H. J.; Subotkowski, W. *J. Am. Chem. Soc.* **1994**, *116*, 7088–7093. (b) Gajewski, J. J. In *Isotopes in Organic Chemistry*; Buncel, E., Lee, C. C., Eds.; Elsevier: New York, 1987; pp 122–130. (c) Gajewski, J. J.; Conrad, N. D. *J. Am. Chem. Soc.* **1979**, *101*, 6693–6704. (d) Kupzcyk-Subotkowska, L.; Subotkowski, W.; Saunders, W. H., Jr.; Shine, H. J. *J. Am. Chem. Soc.* **1992**, *114*, 3441–3445.

(49) (a) Pawlak, J. L.; Padykula, R. E.; Kronis, J. D.; Aleksejczyk, R. A.; Berchtold, G. A. *J. Am. Chem. Soc.* **1989**, *111*, 3374–3381. (b) Delany, J. J.; Padykula, R. E.; Berchtold, G. A. *J. Am. Chem. Soc.* **1992**, *114*, 1394–1397.

Table 8. Theoretical and Experimental Secondary Tritium KIEs k_H/k_T for **5d** and **1**

compd	RHF/6-31G*	BLYP/6-31G*	experiment[a]
chorismic acid **5d** 5-^{3}H	1.106	1.139	
chorismic acid **5d** 9-$^3H_2$	0.955	1.042	
chorismate **1** 5-^{3}H	1.143	1.295	1.149 ± 0.012
chorismate **1** 9-$^3H_2$	0.921	1.034	0.992 ± 0.012

[a] At 333.15 K in aqueous solution, ref 12.

but both methods predict the same trends for the substituent effects on the lengths of the forming and breaking bonds.

The two carboxylic acid groups in **5b** further loosen the transition structure and lower the activation energy. The additional hydroxyl group in chorismic acid **5d** leads to a slight tightening, consistent with an inductive destabilization of the partial cationic character of the allyl fragment in the transition state.

The predictions about the effect of deprotonation differ sharply between the two methods. Whereas the RHF method predicts a shorter C−O bond (~2.1 Å) and a longer C−C bond (~2.4 Å) in the transition structure, the BLYP methods predicts a highly dissociative transition structure with the forming and breaking bonds of about the same length of 2.7 Å. A charge analysis using the CHELPG method shows differences between the character of the transition structures calculated by the two methods. There is charge transfer of 0.15 electrons from the cyclohexadienyl moiety to the enol pyruvyl moiety by BLYP, as compared to 0.33 electrons from the RHF calculations.[41,43b]

This higher diradicaloid character of the BLYP/6-31G* transition structure is also apparent in the theoretical secondary tritium KIEs, shown in Table 8. A normal KIE is calculated for the C-5 position, associated with the breaking bond, as well as for the C-9 position, associated with the forming bond. This indicates that the force constants of the C-H bending motions at C-9 are even smaller in the transition state than in the sp^2 hybridized reactant, a result of the radical character at this center. Similarly, a large normal SKIE is calculated for the breaking bond, again indicating lower bending force constants, higher radical character and a looser transition state than predicted by the RHF method. For the breaking bond, the SKIE from the RHF calculations is within the experimental error, whereas the BLYP method overestimates the SKIE. The length of the breaking C−O bond in the transition state is therefore close to the value of 2.032 Å calculated by the RHF/6-31G* method. Based on the results from the gas phase RHF and BLYP calculations and from the experimental SKIEs in aqueous solution, the length of the forming bond in the transition state can be estimated to be ~2.6 Å.

As already pointed out, at least two conformations of the substituted cyclohexadienyl ring system, the pseudodiequatorial and the pseudodiaxial conformations, need to be considered for chorismate. The energy difference between these two is predicted to be small for the model systems **5a−c** by both computational methods. This is in agreement with NMR studies, which show that the conformational preference of similar systems can easily be reversed by solvent effects.[17] It has been discussed elsewhere that this situation changes for **5d** and **1**, since an intramolecular hydrogen bond between the hydroxyl group and the side chain carboxylic acid or carboxylate can be formed.[8] Comparison of these results with the results for **5b** and **5c** shows that the strong conformational preference found theoretically and experimentally is almost exclusively due to this hydrogen bond. The same trends are obtained by the BLYP method, although the relative energy of the pseudodiaxial conformation of **5b** is 1.8 kcal/mol (1.2 kcal/mol for **5c**) more favorable than predicted by the RHF method. The energy difference of 0.6 kcal/mol calculated for the two conformers of **5c** is in better agreement with the 65:35 preference for the pseudodiequatorial conformation of 4-*O*-methylchorismate in methanol[13] than the corresponding value from RHF calculations.

The activation energies calculated by the two methods show several interesting differences. As for the model systems **4**, the RHF method overestimates the activation energies whereas the BLYP method underestimates them. Nevertheless, the relative activation energies, are similar by the two methods. E_a^{rel}, the activation energies relative to the parent system **4a**, are discussed here. The stabilization of the transition state by the cyclohexadienyl ring in **5a** leads to a decrease of the activation energies by 3−4 kcal/mol. This is in reasonable agreement with the difference of 3.8 kcal/mol in the free energies of activation measured for **4a** and **5a**.[14a] For **5b**, both methods predict a E_a which is 2−3 kcal/mol lower than the activation energy of **4a**, again in good agreement with the experimental value of −2.8 kcal/mol.[14a] For chorismic acid **5d**, a E_a^{rel} of +3.0 kcal/mol is predicted, which is in contrast to the experimental value of −2 kcal/mol. This reflects the stabilization of the pseudodiequatorial ground state in the gas phase by an intermolecular hydrogen bond. In polar solvents, this hydrogen bond is bridged by solvent molecules, and considerable amounts of the pseudodiaxial conformation are present.[13] If the energy difference between the two conformers of **5d** is considered, the E_a^{rel} with respect to the pseudodiaxial conformer is −2.7 kcal/mol, in accordance with the experimental value of −2.0 kcal/mol. Unfortunately, no comparable experimental data are available for the dianion **5c**. The factors influencing the activation energy of **5c**[8] also apply to **1**. A comparison of the results for **5c** and **1** reveals the importance of the intramolecular hydrogen bond on the conformational equilibrium and, therefore, on the computed gas phase activation energy.

Although the general trends in the relative activation energies and SKIEs for **5b−d** and **1** obtained by the RHF and the BLYP method are the same, the values of E_a^{rel} predicted by BLYP are lower by about 5−7 kcal/mol lower than the ones calculated by RHF. From the computed SKIEs, it can be deduced that the BLYP transition structures have a stronger dissociative character. These trends are generally more pronounced for the anionic species **5c** and **1**.

Unfortunately, there are no experimental data available for the model systems **4** and **5** in the gas phase. Furthermore, the influence of polar solvents on the transition structures of charged species is difficult to estimate. The results for the SKIEs and E_a^{rel} from the RHF calculations are in better agreement with the experimental data obtained in polar solvents than the DFT calculations. Since there is also some uncertainty about the performance of density functional methods for the description of hydrogen bonding[50] and other noncovalently bound complexes,[51] the RHF method has been used for all further studies. It remains to be determined in further work using solvent models[52] and other functionals such as the hybrid Becke3LYP functional whether the differences between the RHF and BLYP results are due to solvation effects or due to an unbalanced

(50) For early results of the calculation of hydrogen bonds by DFT methods, see: (a) Hill, R. A.; Labanowski, J. K.; Heisterberg, D. J.; Miller, D. D. In *Density Functional Methods in Chemistry*; Labanowski, J. K., Andzelm, J. W., Eds.; Springer: New York, 1991; pp 357−372. (b) Sim, F.; St-Amant, A.; Papai, I.; Salahub, D. R. *J. Am. Chem. Soc.* **1992**, *114*, 4391−4400. (c) Gresh, N.; Leboef, M.; Salahub, D. R. In *Modelling the Hydrogen Bond*; Smith, D. A., Ed.; ACS Symposium Series 569; American Chemical Society: Washington DC, 1994; pp 82−112.

(51) Ruiz, E.; Salahub, D. R.; Vela, A. *J. Am. Chem. Soc.* **1995**, *117*, 1141−1142.

(52) Davidson, M. M.; Hillier, I. H.; Hall, R. J.; Burton, N. A. *J. Am. Chem. Soc.* **1994**, *116*, 9294−9297.

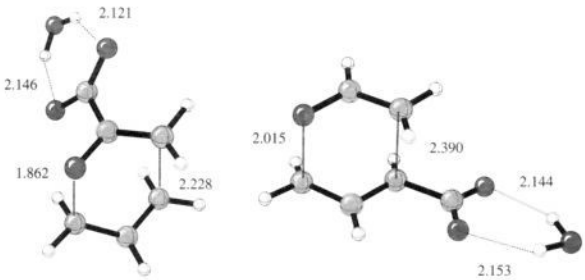

Figure 7. Transition structures for **6** (left) and **7** (right) (RHF/6-31+G*).

Table 9. Results for Model Systems **6** and **7** (RHF/6-31+G*)

model system		reactant	transition structure	Δ, [kcal/mol]
6	E	−531.75264 h	−531.68714 h	41.5
	E_{rel}[a]	−14.9 kcal/mol	−14.3 kcal/mol	0.6
7	E	−531.75712 h	−531.69315 h	40.1
	E_{rel}[a]	−13.2 kcal/mol	−13.6 kcal/mol	−0.4

[a] Relative to the separated molecules, not corrected for BSSE.

description of the dissociative character of the transition state by the BLYP method.

Model Systems for Catalysis of the Claisen Rearrangement

Results and Discussion. The three-dimensional structure of the active site of chorismate mutase from *B. subtilis* (Figure 4) shows numerous contacts between amino acid side chain and the transition state analog, **3**. The relative importance of these contacts was evaluated by studying the influence of the interaction of several functional groups on the activation energies of the model systems, **4a**−**g**. The functional groups have been chosen to mimic the hydrogen bonding interactions of the carboxylates as well as the interactions of the cyclohexadienyl and enol pyruvyl moieties with external groups.

The role of the hydrogen bond between Tyr-108 and the side chain carboxylate at C-10, was modeled by calculating the interaction of allyl vinyl ether-2-carboxylate **4c** with a water molecule. The model system **6** is shown in Figure 7. Similarly, **7** was studied as a model for the interaction of the water molecule in the active site with the ring carboxylate at C-11 of chorismate using the RHF/6-31+G* method.[53] Comparison of the geometries of the calculated transition structures of systems **6** and **7** with the geometries calculated for **4c** and **4e**, respectively, show that the complexation of a water molecule has no significant effect on the lengths of the forming and breaking bonds. The bond lengths calculated for the hydrogen bonds are also in the range typical for the interaction of a water molecule with a carboxylate.[54] The results for the interaction and activation energies for **6** and **7** are summarized in Table 9. The double hydrogen bonding of a water molecule to the carboxylate stabilizes the reactant and transition structure equally by approximately 16.5 kcal/mol. This strong hydrogen bonding is characteristic of a charged system in a nonpolar environment. Therefore, the activation energies computed for **6** and **7** are virtually identical to the activation energies of the uncomplexed systems **4c** and **4e**, respectively. It is clear that hydrogen bonding to one carboxylate at a time has no catalytic effect.

The strong interaction energy of hydrogen bonding at both carboxylates might be used to overcome the electrostatic repulsion of the two negative charges in the transition state of the reaction of a dicarboxylate. A model system was studied to determine how much selective transition state stabilization might be achieved by hydrogen bonding optimized for the transition state of the reaction. The model system is **8**, with two water molecules hydrogen bonding to the carboxylates of allyl vinyl ether−2,6-dicarboxylate, **4g**. To locate the optimal positions for the water molecules in the transition state, the transition structure **8a** was calculated first. As with model systems **6** and **7**, the two water molecules have virtually no effect on the lengths of the forming and breaking bonds as compared to **4g**. The lengths of the hydrogen bonds are close to the values calculated for **6** and **7**. In the next step, the relative positions of the two water molecules were fixed, and reactant **4g** was docked in and optimized. In order for **4g** to achieve hydrogen bonding to both water molecules, the reactant adopts the conformation, **8b**, shown in Figure 8. Because of the selective binding of the reactant in a conformation that resembles the transition state more, the activation energy of the reaction is lowered to 45.3 kcal/mol, 6 kcal/mol less than for the corresponding reaction of **4g** in the absence of the water molecules (51.3 kcal/mol at the RHF/6-31G* level). The fact that the catalytic effect results from the selective binding the transition state is illustrated by the results from the calculation of the fully optimized reactant, **8c**. Here, the constraints on the position of the two water molecules have been removed. Consequently, the reactant adopts an extended conformation similar to the reactant conformation of **4g**. This conformation is 6.9 kcal/mol lower in energy than **8b**, and the activation energy from **8c** to **8a** is now very close to the activation energy of **4g**. This model calculation demonstrates another phenomenon observed in the enzyme and the antibody 1F7: in a catalytic site optimized for transition state binding, the reactant is bound into a transition state-like conformation.

It has been proposed in the literature[24,27] that the phenyl group of Phe-57 might catalyze the Claisen rearrangement of chorismate by stabilizing the positive partial charge in the cyclohexadienyl part of the transition state and by polarization of the transition state. Based on earlier results,[8] this effect is expected to be small, since the charge transfer between the cyclohexadienyl and the enol pyruvyl moieties in the transition structure of **1** is only 0.35 electron. To establish an upper limit on this interaction, the transition state stabilization of allyl vinyl ether **4a** by an extremely polarizing ion, the hydride anion, was calculated in model system **9** using the RHF/6-31+G* method. As shown in Figure 9, the hydride anion was positioned 3.0 Å below the allylic part of **4a**.[55] The transition structure calculated is much looser than the one calculated for **4a** at the same level of theory with the forming and breaking bond elongated by ~0.2 Å. It has a negative partial charge of 0.58 e^- (CHELPG, RHF/6-31+G*) in the oxallylic part and is therefore considerably more polarized than **4a**, where 0.35 electron has been transferred from the allylic to the oxallylic part. Despite this strong effect on the geometric and electronic structure, the activation energy is lowered by only 2.3 kcal/mol by the hydride ion. Since the effect of the uncharged phenyl is expected to be much smaller, it can be concluded that the effect will be negligible. A stationary point for the interaction of benzene with the transition structure of **4a** could not be located.

(53) We have also studied **6** and **7** using the RHF/6-31G* method. In accordance with the results for **4a**−**g**, no significant differences to the RHF/6-31+G* results have been found. We therefore conclude that the RHF/6-31G* method gives an appropriate description of the interactions of the carboxylates with water molecules.

(54) Isaacs, N. S. *Physical Organic Chemistry*; Longman: Harlow; 1987; pp 62−67.

(55) Due to the constrained position of the hydride anion, the calculated transition structure of **9** has three negative eigenfrequencies. One corresponds to the reaction coordinate of the Claisen rearrangement, while the other two refer to movements of the hydride parallel and perpendicular to the allyl plane.

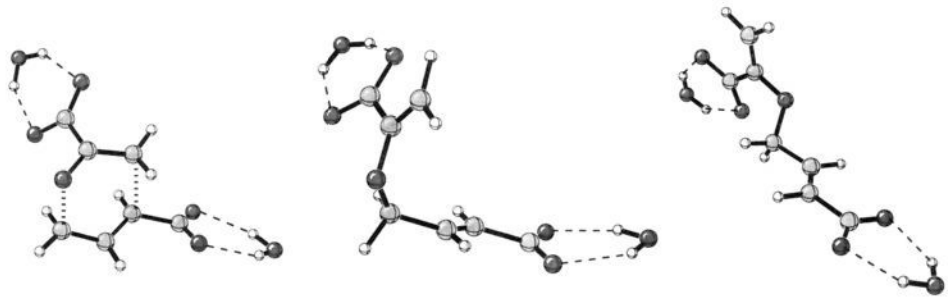

Figure 8. Transition structure **8a** (left), constrained reactant **8b** (middle), and relaxed reactant **8c** (right) for allyl vinyl ether−2,6-dicarboxylate with two hydrogen bonded water molecules (RHF/6-31G*).

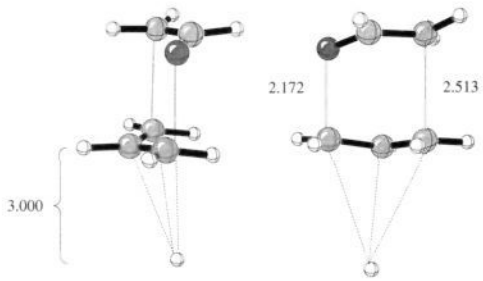

Figure 9. Geometry of the transition structure of **9** (RHF/6-31+G*).

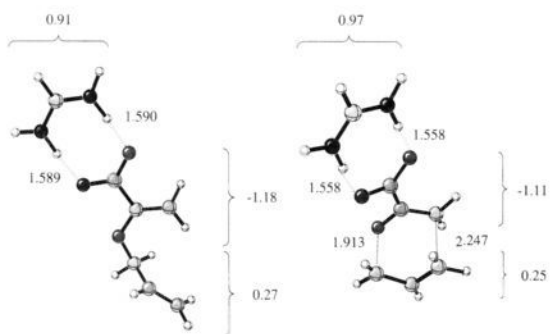

Figure 10. Geometry and partial charges for the reactant (left) and transition structure (right) of **10** (RHF/6-31G**).

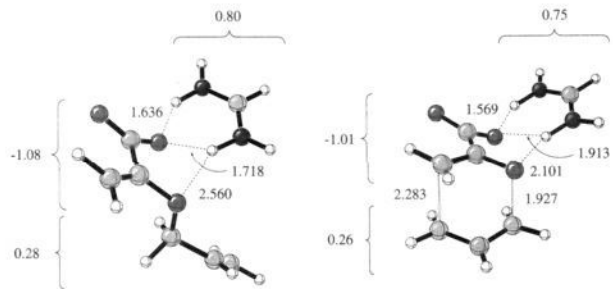

Figure 11. Geometry and partial charges for the reactant (left) and transition structure (right) of **11** (RHF/6-31G**).

The two arginines, Arg-7 and Arg-90, of *B. subtilis* chorismate mutase provide a highly positively charged area of the active site and are complementary to the negatively charged side chain carboxylate and the ether oxygen. While Arg-7 has contacts to both carboxylate oxygens, Arg-90 binds to the ether oxygen and one of the carboxylate oxygens. To mimic these interactions, the model systems **10** and **11** (shown in Figures 10 and 11) were studied using the RHF/6-31G** method. High level calculations of the amidine-formic acid dimer show that in the gas phase, the neutral dimer is favored over the ion pair form.[56] Based on the pH profile of the reaction,[25] it can be assumed that the ion pair form is present in the active site. Therefore, only the ion pair form has been considered, and the N−H bond lengths of the hydrogen-bonded hydrogens were constrained to 1.072 Å to prevent proton transfer in the calculation.[57]

The complexation of the amidinium cation to the carboxylate in **10** has only a small effect on the transition structure geometry. The forming and breaking bonds are elongated by 0.04 and 0.07 Å, respectively, as compared to the uncomplexed **4c** at the same level of theory. The cation is tightly bound to the anion. The O−H(N) distance, indicative of the strength of the hydrogen bond formed between the ions, is very similar in the reactant (1.59 Å) and in the transition structure (1.56 Å). The cation provides charge complementarity to the carboxylate anion. Because of the higher polarizability of transition states, 0.13 electron is transferred through the hydrogen bond to the amidinium cation in the transition structure calculated for **10**, compared to only 0.09 electrons in the reactant. This leads to a lowering of the activation energy by 1.7 kcal/mol. There was no significant catalytic effect calculated for the corresponding model system **6**, which has only hydrogen bonding to water, but no positive charge. Based on these results, it can be concluded that the catalytic effect of the amidinium cation is due to the charge transfer interaction in the ion pair. It has already been discussed that the electrostatic repulsion of the two carboxylates in **1** leads to an increase in the activation energy. It can therefore be expected that the catalytic effect of an amidinium complexed to the carboxylate will be even larger for dianions like **1** or **4g**.

Model system **11** mimics the interaction of Arg-90, the bridging amidinium cation. This arrangement results in a slightly larger effect. The bond lengths of the forming and breaking bonds in the calculated transition structure are now increased by about 0.08 Å. The hydrogen bonding pattern between the amidinium and the oxallyl moiety changes drastically between the reactant and the transition structure. In the reactant, the two hydrogen bond distances to the carboxylate oxygen are approximately equivalent (1.72 and 1.64 Å), whereas the hydrogen bond to the ether oxygen is very weak (2.56 Å). In the calculated transition structure, the latter hydrogen bond is much shorter (2.10 Å), causing one of the hydrogen bonds to the carboxylate oxygen to be elongated to 1.91 Å, whereas the other one is shortened to 1.57 Å. In the reactant, 0.20 electron is transferred to the cation as compared to 0.25 electron in the transition structure. The partial charge of the oxallyl part, however, remains essentially constant. It appears therefore that the calculated lowering of the activation energy of 2 kcal/mol as compared to the uncomplexed system is largely due to improved hydrogen bonding of the amidinium cation to the ether oxygen.

(56) Agranat, I.; Riggs, N. V.; Radom, L. *J. Chem. Soc., Chem. Commun.* **1991**, 80−81.

(57) This value results from optimizations of the guanidinium−formate dimer at the RHF/6-31G** level.

This effect has been discussed in the literature in connection with the catalysis of the Claisen rearrangement of allyl vinyl ether by water. The solvent effect has been studied experimentally[58] and theoretically[59] using a variety of methods. In order to study the effect of a single water molecule hydrogen bonded to the ether oxygen, model system **12** was calculated. Compared with the RHF/6-31G** results for uncomplexed **4a**, the transition structure in **12** is looser by about 0.06 Å. In going from the reactant to the transition structure, the O–H hydrogen bond becomes shorter by 0.164 Å, which is in accordance with the stronger hydrogen bond predicted earlier.[59a] As expected for the complexation of a neutral water molecule to **4a**, no significant changes in the charge distribution pattern are found, and the values are close to the values calculated for parent **4a**. The activation energy calculated for **12** is 43.9 kcal/mol, 2.6 kcal/mol less than for the uncomplexed **4a**. This value is somewhat smaller than the 3.85 ± 0.16 kcal/mol obtained by a Monte Carlo simulation[59a] or the value of 3.5 ± 0.1 kcal/mol from a QM/MM simulation for the reaction in aqueous solution.[59d] These methods, however, do not allow for relaxation of the reactant in the solvent. Solvent/solute polarizations are taken into account in a recent semiempirical SCRF study, which yields transition state stabilizations between 1.6 and 2.0 kcal/mol.[59c] Furthermore, it has been shown that increased bonding by a diaryl urea to the ether oxygen leads to catalysis of a Claisen rearrangement by a factor of 22.[60] From these results, it is clear that the calculated catalysis in **11** is mainly due to improved hydrogen bonding, whereas in the case of **10**, charge complementarity is more important. It remains to be studied whether these factors are additive and how the reaction of a dianion is influenced by the complexation.

Finally, the possiblility of electrophilic catalysis by Arg-90 was investigated. Such catalysis would involve very tight binding of the arginine side chain to, or even protonation of, the ether oxygen. To study the effects of such an interaction, **13** and **14**, shown in Figure 13, were chosen as models. Experimentally, NH_4Cl is a weak heterogeneous catalyst for Claisen rearrangements.[61] Although the catalysis of the aromatic Claisen rearrangement by Brønsted acids is well studied, little is known about the catalysis of aliphatic Claisen reactions.[62] In Lewis or Brønsted acid catalyzed reactions, cleavage of the ether is a common, sometimes dominant, side reaction.[61,63]

The results from the RHF/6-31G** calculations are summarized in Table 12. As in **11** and **12**, the ammonium cation in **13** binds much more tightly to the ether oxygen in the transition structure than in the reactant. This leads also to a considerable polarization of the transition structure. Although the positive charge remains essentially centered at the ammonium cation, the oxallyl part has much more negative partial charge in the transition structure than in the reactant, leading to a positive partial charge of +0.55 electron in the allyl part of the molecule. Because of the stronger coordination in the transition structure of **13**, the breaking bond is calculated to be 0.232 Å longer than in **4a** at the same level of theory. The forming bond is elongated even more (0.317 Å), so that the overall character of the transition structure approaches a dissociative mechanism. By these effects, the activation energy is lowered by 11.4 kcal/mol as compared to **4a** at the same level of theory. The trends calculated for **13** are much more pronounced in the protonated allyl vinyl ether **14**. Here, an extremely loose transition structure with bond lengths for the forming and breaking bonds of 2.57 and 3.07 Å, respectively, is obtained. Due to the higher polarizability of the transition state, a high amount of charge is transferred from the allyl part of the molecule to the proton. Although the activation energy is lowered by 39.3 kcal/mol, the calculated transition structure has to be described as a loose complex between an enol and an allyl cation. It has been pointed out that in solution, this essentially free allyl cation will be highly susceptible to nucleophilic substitution.[15,64]

Table 10. Results for the Model Systems **10** and **11** (RHF/6-31G**, CHELPG)

model system	E + ZPE [h]	E_a [kcal/mol]
4c + amidinium cation[a]	−605.12914	45.1
10	−605.32222	43.4
11	−605.30936	43.1

[a] Separated molecules, not corrected for BSSE.

Table 11. Results for Model System **12** (RHF/6-31G**)

model system	E + ZPE [h]	E_a [kcal/mol]
4a + water[a]	−344.68062	45.1
12	−344.68565	43.9

[a] Separated molecules, not corrected for BSSE.

Table 12. Results for Model Systems **13** and **14** (RHF/6-31G**)

	13		14	
	reactant	TS	reactant	TS
E [h]	−325.20732	−325.15131	−268.99300	−268.98379
$E_{a\,[kcal/mol]}$		35.2		5.8
R_{O-H} (Å)	1.689	1.432	0.954	0.946
δ NH_4^+ (H^+)	0.83	0.85	0.45	0.45
δ oxallyl part	−0.16	−0.40	0.02	−0.32
δ allyl part	0.33	0.55	0.53	0.87

Comparison with the Chorismate Mutase from *Escherichia coli*

After the completion of this study, the three-dimensional structure of a bifunctional chorismate mutase from *E. coli* was published.[29a] The active site is shown in Figure 14. Although there is only 17% sequence homology between the two chorismate mutases from *B. subtilis* and *E. coli* and the secondary structures are very different, the interactions observed in the active site of the *E. coli* chorismate mutase are in good agreement with the results from our calculations. Since the inhibitor is completely buried in the enzyme, there are even more contacts found in the active site. The bonding of the reactant in a transition state-like conformation is achieved by an extensive hydrogen bond network involving the side chains

(58) (a) Gajewski, J. J. *J. Org. Chem.* **1992**, *57*, 5500–5506. (b) Gajewski, J. J.; Brichford, N. L. In *Structure and Reactivity in Aqueous Solution*; ACS Symposium Series 568; Cramer, C. J., Truhlar, D. G., Eds.; American Chemical Society: Washington, DC, 1994; pp 229–242.

(59) (a) Severance, D. L., Jorgensen, W. L. *J. Am. Chem. Soc.* **1992**, *114*, 10966–10968. For an overview on the methods used see: (b) Severance, D. L.; Jorgensen, W. L. In *Structure and Reactivity in Aqueous Solution*; ACS Symposium Series 568; Cramer, C. J., Truhlar, D. G., Eds.; American Chemical Society: Washington, DC, 1994; pp 243–259. (c) Storer, J. W.; Giesen, D.; J. Hawkins, G. D.; Lynch, G. C.; Cramer, C. J.; Truhlar, D. G.; Liotard, D. A. In *Structure and Reactivity in Aqueous Solution*; ACS Symposium Series 568; Cramer, C. J., Truhlar, D. G., Eds.; American Chemical Society: Washington, DC, 1994; pp 24–49. (d) Gao, J.; Xia, X. In *Structure and Reactivity in Aqueous Solution*; ACS Symposium Series 568; Cramer, C. J., Truhlar, D. G., Eds.; American Chemical Society: Washington, DC, 1994; pp 212–228.

(60) Curran, D. P.; Kuo, L. H. *Tetrahedron Lett.*, **1995**, *36*, 6647–6650.

(61) (a) Ziegler, F. E. *Chem. Rev.* **1988**, *88*, 1423–1452. (b) Ralls, J. W.; Lundin, R. E.; Bailey, G. F. *J. Org. Chem.* **1963**, *28*, 3521–3526.

(62) For a review see: Lutz, R. P. *Chem. Rev.* **1984**, *84*, 206–247.

(63) E.g.: Borgulya, T.; Madeja, R.; Gahrni, P.; Hansen, H.-J.; Schmid, H. *Helv. Chim. Acta* **1973**, *56*, 14–75.

(64) DeWolfe, R. H., Young, W. G. *Chem. Rev.* **1956**, *56*, 753–901.

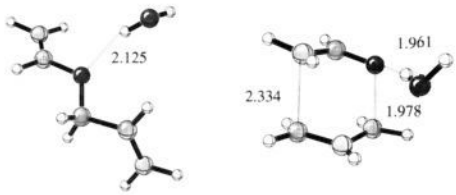

Figure 12. Geometry and partial charges for the reactant (left) and transition structure (right) of **12** (RHF/6-31G**).

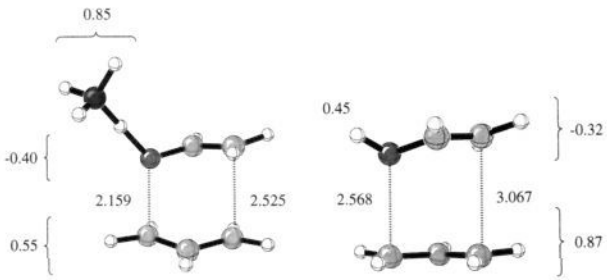

Figure 13. Geometry and partial charges for the transition structures for **13** (left) and **14** (right) (RHF/6-31G**).

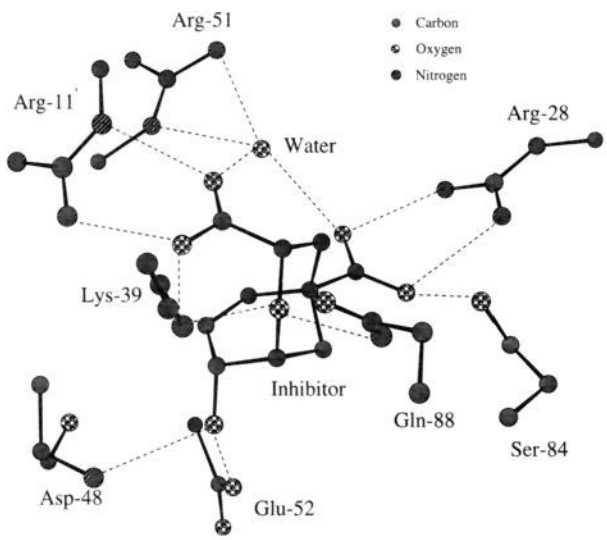

Figure 14. Active site of chorismate mutase from *Escherichia coli*.[29a]

of Arg-28, Arg-51, Arg-11′, Lys-39, and Ser-84. There are no inhibitor-side chain contacts suitable for the stabilization of a positive partial charge in the cyclohexadienyl part of the transition state, in accordance with our findings that such an interaction would be unimportant for catalysis. Charge complementarity in the active site is provided by Arg-11′ and Lys-39 (as compared to Arg-7 and Arg-90 in the chorismate mutase from *B. subtilis*) with arrangements very similar to our model systems. The ether oxygen is even more strongly bound by two hydrogen bond interactions with Lys-39 and Gln-88. It is noteworthy that although the structural motifs of the two enzymes are different, the mode of catalysis represented in the model systems studied here is similar. It can therefore be expected that there could be a variety of different arrangements giving a similar catalytic effect.

Conclusions

The substituent effects of the various functional groups present in chorismate **1** have been explored through calculations on the model systems **4** and **5** at different levels of theory. The results are in reasonable agreement with the available experimental data. Substitution of allyl vinyl ether by a carboxylic acid group in 2-position accelerates the reaction, whereas substitution in 6-position increases the activation energy. Deprotonation of the acids to the corresponding anions lowers the activation energy substantially by interaction of the charge with the more polarizible transition state, suggesting a more general mode of catalysis for pericyclic reactions. Whereas the substituent effect of the carboxylic acid group on the geometry of the calculated transition structure is small, deprotonation leads to a looser transition structure in case of substitution on 2-position and to a tighter one for the 6-carboxylate **4e**. The effects are roughly additive for the dianion, although electrostatic repulsion leads to a much higher activation energy for the dianions. The cyclohexadienyl group in the model systems **5** leads to a generally looser transition structure. As has been shown earlier for chorismate **1**,[8] the conformational equilibrium and the activation energies calculated for model compounds **5** is dependent on intramolecular hydrogen bonding.

The results from the calculations of the model systems **6**−**14** provide information about how the native enzyme chorismate mutase catalyzes a pericyclic reaction by a factor of about 2×10^6. The different factors that are important for catalysis can be separated out by the computations. Based on these results, the most important factor is the selective transition state binding, resulting in a lowering of the activation energy by about 6 kcal/mol. This is achieved by the stronger binding (as compared with the aqueous solution) of the enol pyruvyl side chain by Arg-7 and Arg-90. The arrangement is particularly complementary to the transition state conformation. The second effect of the arginines is the charge complementarity of Arg-7 to the carboxylate and the hydrogen bonding of Arg-90 to the ether oxygen. Stronger binding to the ether oxygen as in the case of electrophilic catalysis results in a dissociative transition structure, which is not in accord with the experimental results. Compared to these effects, the influence of a potential stabilization of the positive partial charge in the cyclohexadienyl part of the molecule is negligible, as can be deduced from the calculations of model system **9**. This is also in agreement with the fact that although the reaction of 2,3-dihydrochorismate is slower than the reaction of chorismate, the rate acceleration by chorismate mutase is very similar for both compounds.[49]

The results also provide additional insights into the reasons for the lower catalytic activity of the antibody 1F7. Although the active site also forces the substrate into a transition state-like conformation, the binding interactions are much weaker as compared to the enzyme. As can be seen in Figure 5, the interactions to the ether oxygen and the side chain carboxylate, which are found to be important for catalysis by our calculations, are contacts with the backbone of the protein. The side chains and functional groups of the residues AsnH33, AspH99, and ArgH95 are pointing away from the active site. Therefore, there are no functional groups present in the active site that could provide the charge complementary or increased hydrogen bonding found to be important for catalysis. Furthermore, an improvement of the catalytic antibody by site directed mutagenesis would require significant changes in the backbone conformation to allow the interaction of suitable functional groups with the relevant moieties of the transition state.

Acknowledgment. We are grateful to the National Science Foundation for financial support of this research and the UCLA Office of Academic Computing for computer time and facilities. O.W. thanks the Alexander von Humboldt Foundation (Germany) for a Feodor Lynen Fellowship. We thank Professor Donald Hilvert and Professor William N. Lipscomb

for the communication of results prior to publication. Valuable discussions with Professor Donald Hilvert are also acknowledged.

Supporting Information Available: Energies, zero point energies, imaginary frequencies and Cartesian coordinates of all structures (34 pages). This material is contained in many libraries on microfiche, immediately follows this article in the microfilm edition of the journal, can be ordered from the ACS, and can be downloaded from the Internet; see any current masthead page for ordering information and Internet access instructions.

JA951905T